Local-cosine beamlet migration for 3D complex structures

Ru-Shan Wu, Yongzhong Wang*, Mingqiu Luo,
Modeling and Imaging Laboratory, IGPP, University of California, Santa Cruz, CA, 95064
*presently Geophysical Development Corporation, Houston, TX 77001

This paper was prepared for presentation at the 8th International Congress of The Brazilian Geophysical Society held in Rio de Janeiro, Brazil, 14-18 September 2003.

Abstract

3D poststack and prestack depth migrations using the local cosine basis (LCB) beamlet propagator are applied to the synthetic data sets of 3D SEG/EAGE salt model. Beamlet propagator is decomposed into a beamlet free-propagator and a local perturbation operator. The results of poststack migration show good image quality not only for the salt boundaries, but also for the subsalt structures. For prestack migration, the imaging is implemented in the shot domain. Both the source field and the receiver array field are decomposed into LCB beamlets and sinked down to image levels using beamlet propagators. Imaging condition can be applied either in beamlet domain or space domain. The data used are the 45 shots synthetic data set of the salt model. The results demonstrate the high resolution and high quality feature of the beamlet migration, that can be seen clearly from the images of the highly irregular top salt boundary.

Introduction

Many dual domain (space-wavenumber domain) propagators have been developed for wave propagation and imaging in complex media, such as FFD (Ristow et al., 1994) and GSP(Wu, 1994, Jin et al., 1998, Xie and Wu, 1998, Huang et al., 1999, Xie and Wu, 1999; Xie et al., 2000; De Hoop et al., 2000). In such methods, the medium is decomposed at each level into a global background (reference) medium and global perturbations to account for lateral velocity variations. For strong contrast media, the perturbation can be very large leading to difficulties in correctly and efficiently propagating large-angle waves. Some authors (Steinberg, 1993; Steinberg and Birman, 1995) attempted to develop local phase-space propagators using the windowed Fourier Transform (WFT) instead of the traditional global propagators. However, the reference velocity and perturbations were still global in their method. Other authors (Wu and Jin, 1997; Jin and Wu, 1999) tried to use the WFT for localizing the generalized screen propagator, in which local reference velocities were used. However, windowed screen propagator method can be applied only to media with a few boundaries and did not represent general localized propagators. Wu et al. (2000) proposed beamlet migration methods based on local reference velocity and local perturbation theory using Gabor-Daubechies frame (GDF) and local cosine basis (LCB). The methods have been applied to 2D SEG/EAGE salt model and Marmousi data sets (Wu et al., 2000, 2002; Chen and Wu, 2002; Wu and Chen, 2001; Wang and Wu, 2002). In this work, we extend the LCB beamlet propagator to 3D poststack and prestack depth migration and test the algorithms with the synthetic data set generated by explode reflection modeling for the poststack data and the Sandia's 45 shots data set for prestack data of the 3D SEG/EAGE salt model. We compare its result with that of FD, and discuss the accuracy and efficiency of the method.

3D beamlet migration

In frequency-space (f-x) domain, the scalar equation can be written as,

$$[\partial_x^2 + \partial_y^2 + \partial_z^2 + \omega^2 / v^2(x,y,z)]u(x,y,z,\omega) = 0 \,. \quad (1)$$

Here, u stands for wave field, $v(x,y,z)$ stands for velocity function. The wave field at depth z can be decomposed into beamlets with windows along the x-axis and y-axis,

$$\begin{aligned} u_z(x,y) &= \sum_n \sum_m \sum_p \sum_q < u_z(x,y), \tilde{b}_{mnqp}(x,y) > b_{mnqp}(x,y) \\ &= \sum_n \sum_m \sum_p \sum_q \hat{u}_z(\bar{x}_n, \bar{y}_p, \bar{\xi}_m, \bar{\eta}_q) b_{mnqp}(x,y) \quad (2) \end{aligned}$$

where $b_{mnqp}(x,y)$ are the decomposition atoms, $\hat{u}_z(\bar{x}_n, \bar{y}_p, \bar{\xi}_m, \bar{\eta}_q)$ are the coefficients of the decomposition located at space locus $(\bar{x}_n, \bar{y}_p)$ and wavenumber locus $(\bar{\xi}_m, \bar{\eta}_q)$, and

$$\bar{x}_n = n\Delta x, \quad \bar{y}_p = p\Delta y, \quad \bar{\xi}_m = m\Delta\xi, \quad \bar{\eta}_q = q\Delta\eta \,.$$

For a beamlet at $(\bar{x}_n, \bar{y}_p)$, we can introduce local reference velocity and local perturbations to get its evolution equation,

$$a_{mnqp}(x,y) = e^{\pm i A_{np}\Delta z} b_{mnqp}(x,y) \,. \quad (3)$$

Here a_{mnqp} is a function evolved from b_{mnqp} propagating in the heterogeneous medium and

$$A_{np} = \sqrt{\partial_x^2 + \partial_y^2 + k_0^2(\bar{x}_n, \bar{y}_p, z) + \Delta k_{np}^2(x,y,z)} \,, \quad (4)$$

with $\Delta k_{np}^2(x,y,z) = k^2(x,y,z) - k_0^2(\bar{x}_n, \bar{y}_p, z)$ as the local perturbation with respect to the local reference velocity $v_0(\bar{x}_n, \bar{y}_p, z)$ and $k_0 = \omega / v_0$.

The wave field at depth $z + \Delta z$ can be calculated as

$$\begin{aligned} u_{z+\Delta z}(x,y) &= \sum_n \sum_m \sum_p \sum_q \hat{u}_z(\bar{x}_n, \bar{y}_p, \bar{\xi}_m, \bar{\eta}_q) a_{mnqp}(x,y) \\ &= \sum_l \sum_j \sum_r \sum_i b_{jlir}(x,y) \sum_n \sum_p P^{(1)}_{lr,np}(x,y) \\ &\quad \cdot \sum_m \sum_q P^{(0)}_{jlir,mqnp} \hat{u}_z(\bar{x}_n, \bar{y}_p, \bar{\xi}_m, \bar{\eta}_q) \end{aligned} \qquad (5)$$

where $P^{(0)}$ and $P^{(1)}$ are the background propagator and perturbation operator. The expressions for $P^{(0)}$ and $P^{(1)}$ can be found in Wang and Wu (2002) for the 2D case. The extension to 3D case is straightforward.

Local cosine basis propagator

For local cosine basis, the atoms can be written as

$$b_{mnpq}(x,y) = \psi_{mn}(x)\psi_{qp}(y) . \qquad (6)$$

Here $\psi_{mn}(x) = \sqrt{2/L_n}\, b_n(x) \cos[\pi(m + \frac{1}{2})(x - \bar{x}_n)/L_n]$,

where $L_n = \bar{x}_{n+1} - \bar{x}_n$ is the nominal length of the window and $b_n(x)$ is the bell (window) function. $\psi_{qp}(y)$ has a similar expression.

Poststack migration results of 3D SEG/EAGE salt model

The data are generated using exploding-reflector modeling by ARCO with a finite difference algorithm. The size of this dataset is *Nx=250*, *dx=40m*, *Ny=250*, *dy=40m*, *Nz=201*, *dz=20m*. The time sampling interval is *8ms* with *501* samples per trace. In our migration implementation, we select the frequency range from *0* to *30 Hz*.

Fig. 1(a) is the velocity model of a vertical section. Fig. 1(b) is the poststack migrated image using 3D local cosine beamlet propagator. From the result, we can see that, the salt top and lower boundaries are imaged correctly, most of the subsalt structures are migrated well except for the steeply dipping reflectory. The base line is also reconstructed and positioned correctly. Fig.2 shows the result for a horizotal slice.

Prestack migration result on 3D SEG/EAGE salt model

We applied LCB migration method to the 45-shots data for 3D SEG/EAGE salt model. The grid size for the model is 676, 676 and 210 grids in x, y and z axis respectively. The distribution of the 45 shots is showed

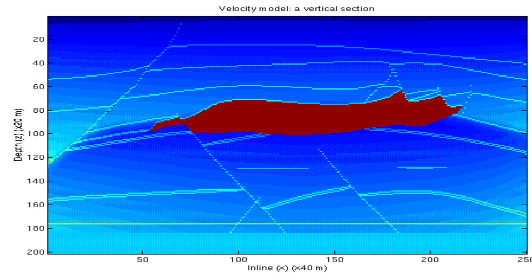

Figure 1 (a): SEG-EAGE C3 salt model for a vertical section.

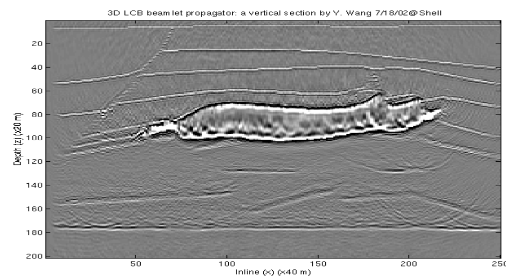

Figure 1(b): 3D poststack migrated image of Fig. 1(a) using the beamlet propagator.

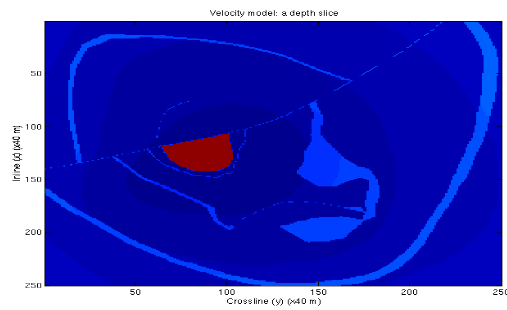

Figure 2(a): SEG-EAGE C3 salt model for a depth slice at *Z=40*.

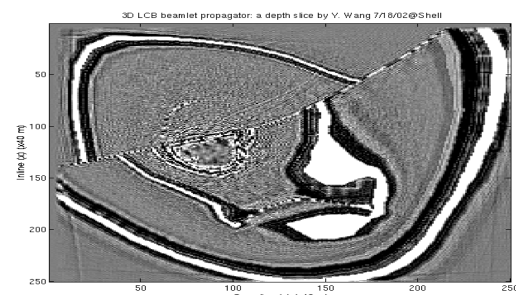

Figure 2(b): 3D poststack migrated image of Fig. 2(a) using the beamlet propagator.

in Fig.3(a). Each shot has a 201×201 receiver grid. The maximum fold is 15. An aperture of 400×400×210 is used in each shot imaging by the LCB method.

We select two slices of the 3D imaging volume as shown in Fig.3(b) and compared with that by finite difference method. Fig. 4 and Fig. 5 give the comparisons of two vertical slices of the migration results respectively. In general, the image qualities of the two methods are similar. However, the LCB images tend to have higher resolution for sharp boundaries, especially for the erratic salt top boundaries. In figure 4, these places are marked with A, B, C and D. Fig.5 shows the enlarged parts of the top salt for detailed comparison. The high resolution and hight image quality can be clearly seen from the comparison. The other feature of LCB beamlet migration is the absence of both numerical dispersion and numerical anisotropy so that the image is less contaminated by dispersion noises.

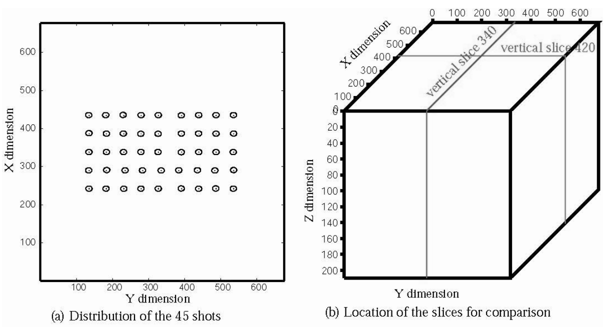

Fig.3 – Distribution of the 45 shots and location of slices for comparison.

Efficiency comparison

Efficiency often plays a key role in the practical use of an imaging method. For LCB method, its efficiency, can be controlled by a parameter which specifies the range of interaction in sparse matrix manipulation. When larger interaction range is adopted, a less efficient but more accurate algorithm is expected.

We compared LCB method with Split-step Fourier (SSF) method in the poststack migration of 3D SEG/EAGE model with 250, 250 and 201 grids in X, Y and Z dimension. LCB method is about 3-4 times slower than SSF method, which is an affordable price we pay for the quality. In prestack migration, LCB method can be more efficient because it only needs to construct the propagator once for both source wavefield and receiver wavefield. There are still potentials to improve the efficiency of the method while keeping superior imaging quality.

Conclusion

Compared to traditional methods, Beamlet migration method with local cosine basis propagator can provide good imaging quality for complex media such as 3D SEG/EAGE model. At present, it is less efficient than the Split-step Fourier method and GSP or FFD method. However, it has its unique features for high resolution, high fidelity imaging. Moreover, there is still potential in improving the imaging quality and efficiency of the method in the future.

Acknowledgements:

The authors would like to acknowledge the support from WTOPI (Wavelet Transform On Propagation and Imaging for seismic exploration) Research Consortium and the DOE/BES project at University of California, Santa Cruz, and thank the Sandia National Lab for the data set and FD migration result.

References

De Hoop, M., Rousseau, J. and Wu, R.S., 2000, Generalization of the phase-screen approximation for the scattering of acoustic waves, Wave Motion, 31, p43-70.

Chen, L. and Wu, R.S., 2002, Target-oriented prestack beamlet migration using Gabor-Daubechies frames, Expanded Abstracts, SEG 72th Annual Meeting, p1356-1359

Huang, L.j., Fehler, M. and Wu, R.S., 1999, Extended local Born Fourier migration method, Geophysics, 64, p1524-1534.

Jin, S., and Wu, R.S., 1999, Depth migration with a windowed screen propagator, Journal of Seismic Exploration, 8(1), 27-38.

Jin S., Wu R.S. and Peng, C., 1999, Seismic depth migration with pseudo-screen propagators, Computational Geosciences, 3, p321-335.

Ristow, D. and Ruhl, T., 1994, Fourier finite difference migration, Geophysics, 59, p1882-1893

Steinberg, B.Z., 1993, Evolution of local spectra in smoothly varying nonhomogeneous environments-local canonization and marching algorithms, J. Acoust. Soc. Am., 93, p2566-2580.

Steinberg, B.Z. and Birman, R., 1995, Phase-space marching algorithm in the presence of a planar wave velocity discontinuity-A qualitative study, J. Acoust. Soc. Am.,98, p484-494.

Wang, Y. and Wu, R.S., 2002, Beamlet prestack depth migration using local cosine basis propagator, Expanded Abstracts, SEG 72th Annual Meeting,p1340-1343

Wu, R.S. and Jin, S., 1997, Windowed GSP (generalized screen propagators) migration applied to SEG-EAEG salt model data, Expanded abstracts, SEG 67th Annual Meeting, 1746-1749.

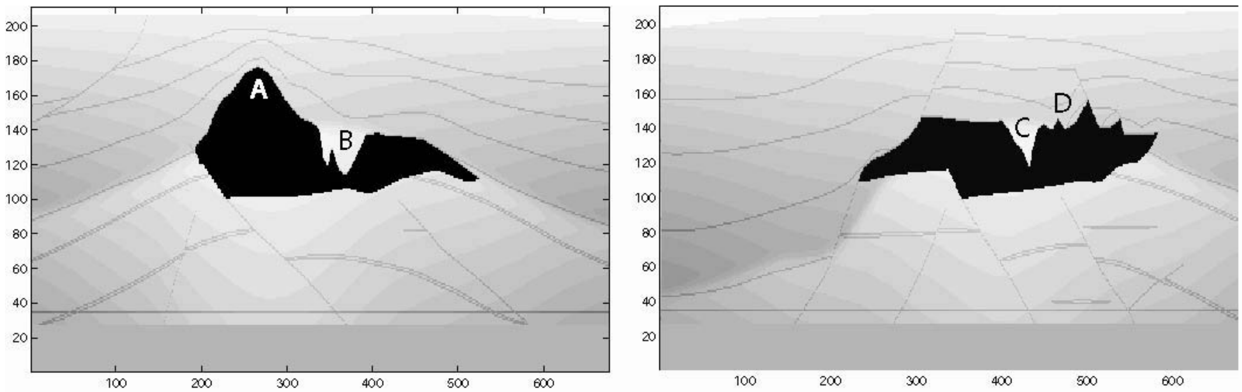

(a) C3 SEG/EAGE salt Model (676X676X210). Left: vertical slice x=420; Right: vertical slice y=340.

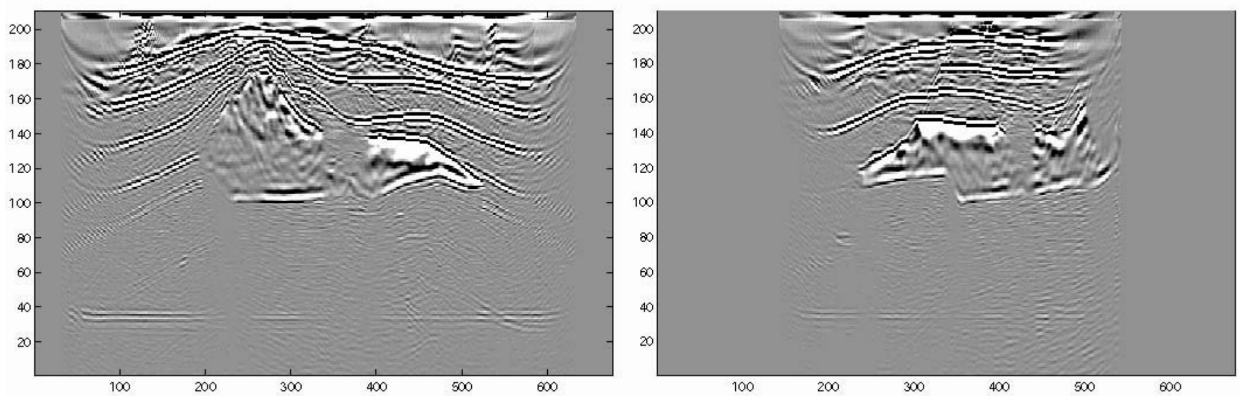

(b) 3D 45 shots prestack depth migration results by Finite Difference method.

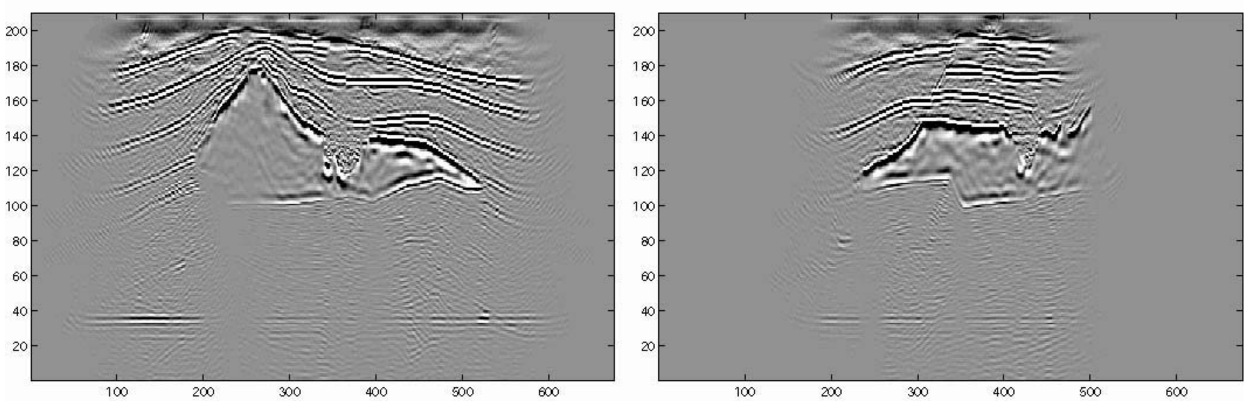

(c) 3D 45 shots prestack depth migration results by LCB beamlet method.

Fig.4 – Comparison of 45 shots prestack depth migartion results (vertical slices) of 3D SEG/EAGE salt model by FD method and LCB beamlet method

Wu, R.S. Wang, Y. and Gao, J.H., 2000, Beamlet migration based on local perturbation theory, Expanded Abstracts, SEG 70th Annual Meeting, p1008-1011.

Wu, R.S. and Chen L., 2001, Beamlet migration using Gabor-Daubechies frame propagator, Expanded Abstracts, EAGE 63th Annual Meeting, p74

Wu, R.S. and Chen, L., 2002, Wave propagation and imaging using Gabor-Daubechies beamlets, “Theoretical and Computational Acousitics”, World Scientific, New Jersey, 666-1-670

Xie, X.B. and Wu, R.S., 1999, Improving the wide angle accuracy of the screen propagator for elastic wave propagation, Expanded abstracts, SEG 69th Annual Meeting, 1863-1866.

Xie, X.B., Mosher, C.C. and Wu, R.S., 2000, The application of wide angle screen propagator to 2D and 3D depth migrations, Expanded abstracts, SEG 70th Annual Meeting, 878-881.

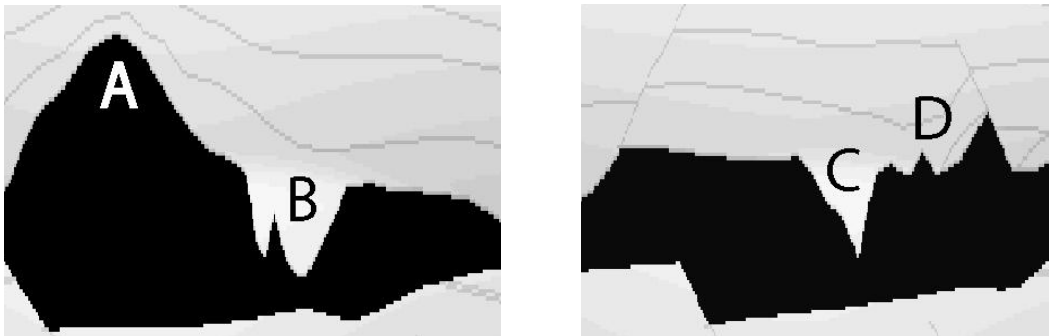

(a) C3 SEG/EAGE salt model (left vertical slice x=420; right vertical slice y=340)

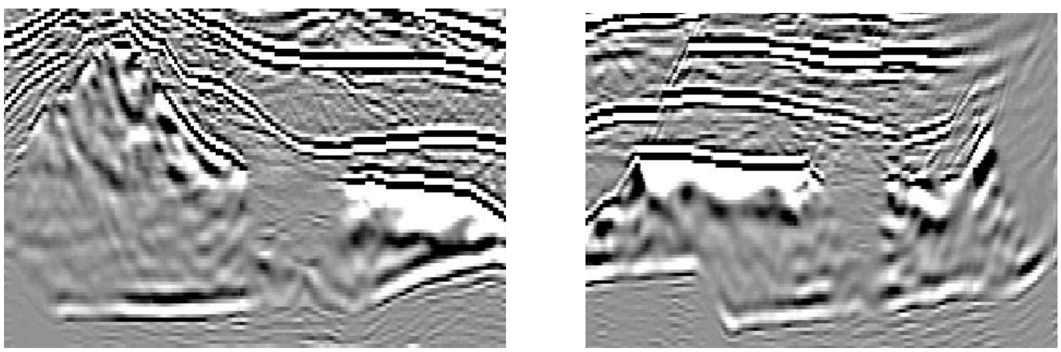

(b) Enlarged images by FD method

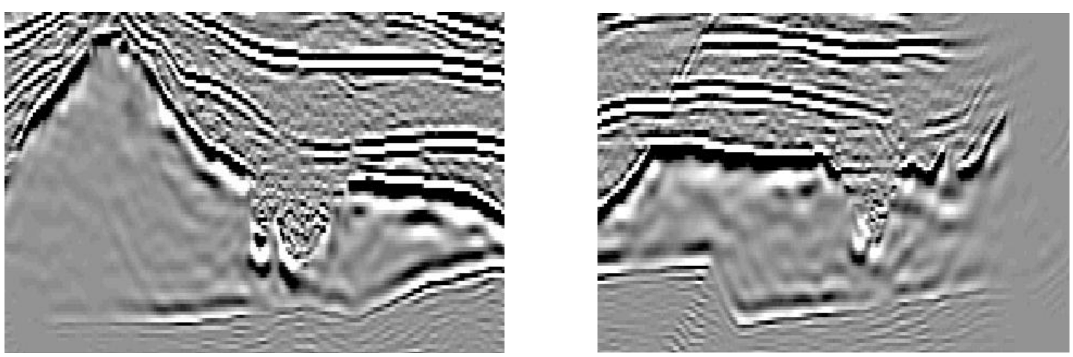

(c) Enlarged images by LCB beamlet method

Fig.5 – Enlarged parts of top salt and their images in Fig.4.